Inorganic Chemistry
Article

Inorg. Chem. **2010**, *49*, 5923–5934 **5923**
DOI: 10.1021/ic100384e

Control of Self-Assembly through the Influence of Terminal Hydroxymethyl Groups on the Metal Coordination of Pyrimidine−Hydrazone Cu(II) Complexes

Daniel J. Hutchinson, Lyall R. Hanton,* and Stephen C. Moratti

Department of Chemistry, University of Otago, P.O. Box 56, Dunedin, New Zealand

Received February 25, 2010

The synthesis and characterization of 6-hydroxymethylpyridine-2-carboxaldehyde (2-methyl-pyrimidine-4,6-diyl)bis(1-methylhydrazone) (**1**) is reported. Ligand **1** was designed as a ditopic pyrimidine−hydrazone molecular strand with hydroxymethyl groups attached to the terminal pyridine rings. Coordination of **1** with $Cu(ClO_4)_2 \cdot 6H_2O$ or $Cu(SO_3CF_3)_2 \cdot 4H_2O$ in a 1:2 molar ratio resulted in the dinuclear Cu(II) complexes $[Cu_2\mathbf{1}(CH_3CN)_4](ClO_4)_4 \cdot CH_3CN$ (**4**) and $[Cu_2\mathbf{1}(SO_3CF_3)_2(CH_3CN)_2](SO_3CF_3)_2 \cdot CH_3CN$ (**5**). X-ray crystallography and ^{1}H NMR NOESY experiments showed that **1** adopted a horseshoe shape with both pyrimidine−hydrazone (pym−hyz) bonds in a *transoid* conformation, while **4** and **5** were linear in shape, with both pym−hyz bonds in a *cisoid* conformation. Coordination of **1** with $Cu(ClO_4)_2 \cdot 6H_2O$ or $Cu(SO_3CF_3)_2 \cdot 4H_2O$ in a 1:1 molar ratio resulted in three different bent complexes, $[Cu(\mathbf{1}H)(ClO_4)_2](ClO_4)$ (**6**), $[Cu(\mathbf{1}H)(CH_3CN)](ClO_4)_3 \cdot 0.5H_2O$ (**7**), and $[Cu\mathbf{1}(SO_3CF_3)]_2(SO_3CF_3)_2 \cdot CH_3CN$ (**8**), where the pym−hyz bond of the occupied coordination site adopted a *cisoid* conformation, while the pym−hyz bond of the unoccupied site retained a *transoid* conformation. Both **6** and **7** showed protonation of the pyridine nitrogen donor in the empty coordination site; complex **8**, however, was not protonated. A variety of Cu(II) coordination geometries were seen in structures **4** to **8**, including distorted octahedral, trigonal bipyramidal, and square pyramidal geometries. Coordination of the hydroxymethyl arm in the mononuclear Cu(II) complexes **6**, **7**, and **8** appeared to inhibit the formation of a [2 × 2] grid by blocking further access to the Cu(II) coordination sphere. In addition, the terminal hydroxymethyl groups contributed to the supramolecular structures of the complexes through coordination to the Cu(II) ions and hydrogen bonding.

Introduction

Supramolecular systems that undergo dynamic structural changes induced by external stimuli are intriguing as they have potential applications as components in nanoscale mechanical devices.[1−3] The pyrimidine−hydrazone (pym−hyz) motif is of interest due to the dynamic structural change of pym−hyz molecular strands from a helical shape to a linear arrangement upon coordination of suitable metal ions.[4−6] Coordination causes the pym−hyz−pym linkage to rotate from the preferred *transoid* conformation to a *cisoid* conformation, which creates a tridentate coordination site for the incoming metal ion (Figure 1). This structural change has been observed when using metal salts of Pb(II),[5] Ag(I),[7] Zn(II),[8] and Hg(II)[9,10] in polar solvents such as CH_3CN and CH_3NO_2, resulting in linear, grid, and double helical complexes. Previous studies have shown that this dynamic process is reversible and that the volume change associated with it is significant.[5]

The key to applying these dynamic molecular systems is their incorporation into devices such as polymer gel actuators, which have potential applications in the fields of biomedical science,[11] robotics,[12] and microfluidics.[13] Our first pym−hyz ligand (**1**) has been designed with terminal 6-hydroxymethyl-2-pyridinecarboxaldehyde rings, which have the

*To whom correspondence should be addressed. Phone: (+64) 3-479-7918. Fax: (+64) 3-479-7906. E-mail: lhanton@chemistry.otago.ac.nz.

(1) Schneider, H.-J.; Strongin, R. M. *Acc. Chem. Res.* **2009**, *42*(10), 1489–1500.
(2) Balzani, V.; Credi, A.; Raymo, F. M.; Stoddart, J. F. *Angew. Chem., Int. Ed.* **2000**, *39*, 3348–3391.
(3) Ulrich, S.; Buhler, E.; Lehn, J.-M. *New J. Chem.* **2009**, *33*, 271–292.
(4) Schmitt, J.-L.; Stadler, A.-M.; Kyritsakas, N.; Lehn, J.-M. *Helv. Chim. Acta* **2003**, *86*, 1598–1624.
(5) Schmitt, J.-L.; Lehn, J.-M. *Helv. Chim. Acta* **2003**, *86*, 3417–3426.
(6) Stadler, A.-M.; Kyritsakas, N.; Graff, R.; Lehn, J.-M. *Chem.—Eur. J.* **2006**, *12*, 4503–4522.
(7) Stadler, A.-M.; Kyritsakas, N.; Vaughan, G.; Lehn, J.-M. *Chem.—Eur. J.* **2006**, *13*, 59–68.
(8) Barboiu, M.; Ruben, M.; Blasen, G.; Kyritsakas, N.; Chacko, E.; Dutta, M.; Radekovich, O.; Lenton, K.; Brook, D. J. R.; Lehn, J.-M. *Eur. J. Inorg. Chem.* **2006**, 784–792.
(9) Ramirez, J.; Stadler, A.-M.; Harrowfield, J. M.; Brelot, L.; Huuskonen, J.; Rissanen, K.; Allouche, L.; Lehn, J.-M. *Z. Anorg. Allg. Chem.* **2007**, *633*, 2435–2444.
(10) Ramirez, J.; Stadler, A.-M. *Z. Anorg. Allg. Chem.* **2009**, *635*, 1348–1351.
(11) Lyon, L. A.; Meng, Z.; Singh, N; Sorrell, C. D.; St. John, A. *Chem. Soc. Rev.* **2009**, *38*, 865–874.
(12) Mirfakhrai, T.; Madden, J. D. W.; Baughman, R. H. *Mater. Today* **2007**, *10*, 30–38.
(13) Becker, H.; Gaertner, C. *Anal. Bioanal. Chem.* **2008**, *390*(1), 89–111.

Published on Web 05/28/2010

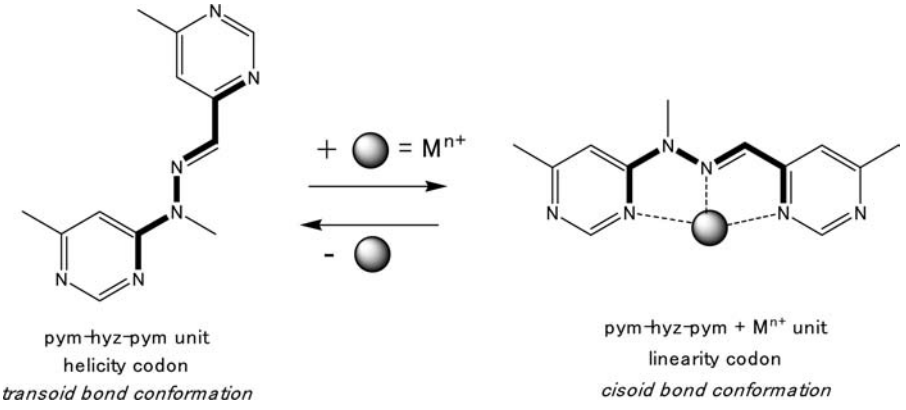

Figure 1. Reversible rotation of the pym−hyz bond from *transoid* to *cisoid* conformation, induced by the addition of metal ions. While the uncoordinated pym−hyz unit acts as a helicity codon, the coordinated pym−hyz + M^{n+} unit imposes a linear shape on the molecular strand.

potential to allow the ligand to be assimilated into larger systems through chemical manipulation of the terminal OH functional groups. While this functionality has been added ultimately to allow incorporation of the ligand strands into molecular devices, the way in which the hydroxymethyl substituents affect the metal coordination chemistry of the pym−hyz strands needs first to be explored. The terminal 6-hydroxymethylpyridine motif may have a direct effect on the self-assembly reaction between the ligand strand and the metal ions by forming a chelate ring with the metal ion through coordination of the N_{py} and O donors.[14−16] It may also alter the supramolecular chemistry of a complex, due to the ability of the OH group to act as both a hydrogen bonding acceptor and donor.[17,18] These attributes have led to the frequent use of the 6-hydroxymethylpyridine motif with Cu(II) ions to create self-assembled supramolecular architectures through a combination of metal coordination and hydrogen bonding.[19−21]

An extensive family of pym−hyz (and isomorphically equivalent pym−py) ligands has been reported with different substituents on the ternary hydrazone N atoms, the 2 position of the pyrimidine ring, and the terminal pyridine rings.[4−6] These modifications have been made to tune the redox[22] and magnetic[23] properties of the pym−hyz complexes, alter the solid state structure of the self-assembled complexes,[6] produce functionalized grids which may be used as sensors,[24] and produce extended 1D and 2D grid assemblies through self-assembly reactions.[25,26] However, few examples exist where the pym−hyz strands have been decorated with OH functional groups,[6] particularly at the terminal pyridine rings where they can influence the metal-directed self-assembly process.

Herein, we report the preliminary metal coordination studies of this new pym−hyz ligand with $Cu(ClO_4)_2 \cdot 6H_2O$ and $Cu(SO_3CF_3)_2 \cdot 4H_2O$ in CH_3CN. The addition of each of the Cu(II) salts to **1** in a 2:1 molar ratio resulted in a linear complex with Cu(II) ions occupying both of the pym−hyz−py coordination pockets of **1**. In both of the dicopper complexes, only one of the terminal hydroxymethyl groups was coordinated to a Cu(II) ion. When the Cu(II) salts were added to **1** in a 1:1 molar ratio, the conformational change of the pym−hyz linkage from *transoid* to *cisoid* was localized to only the occupied pym−hyz−py pocket, while the vacant coordination pocket retained a horseshoe-like shape. Two different solid state structures with differing Cu(II) coordination spheres were obtained from reacting **1** with $Cu(ClO_4)_2$ in a 1:1 molar ratio. In both complexes, the pyridine nitrogen donor of the empty coordination pocket was protonated, while the hydroxymethyl group of the occupied site was bound to the Cu(II) ion. Coordination of the hydroxymethyl arm in these mononuclear Cu(II) complexes appeared to inhibit the formation of a [2 × 2] grid by blocking further access to the Cu(II) coordination sphere.

Experimental Section

General. All chemicals were used as received without further purification. The precursor 4,6-bis(1-methylhydrazino)-2-methylpyrimidine (**2**) was prepared from 4,6-dichloro-2-methylpyrimidine and methyl hydrazine.[27] Activated manganese(IV) dioxide (MnO_2) and 2,6-bis(hydroxymethyl)pyridine were obtained from Merck and Acros Organic, respectively. $Cu(ClO_4)_2 \cdot 6H_2O$ was acquired from Aldrich, while $Cu(SO_3CF_3)_2 \cdot 4H_2O$ was prepared by the treatment of $CuCO_3$ with HSO_3CF_3. All solvents were used as received and were of LR grade or above. The petroleum ether used was the 40−60 variety.

Column chromatography was performed using silica gel (10% hydrated v/v). Microanalyses were carried out in the Campbell Microanalytical Laboratory, University of Otago. All measured microanalysis results had an uncertainty of ±0.4%. ^1H and ^{13}C NMR spectra and two-dimensional (gCOSY, NOSEY,

(14) Winter, S.; Seichter, W.; Weber, E. *Z. Anorg. Allg. Chem.* **2004**, *630*, 434–442.
(15) Yilmaz, V. T.; Guney, S.; Andac, O.; Harrison, W. T. A. *Polyhedron* **2002**, *21*, 2393–2402.
(16) Maroszová, J.; Stachová, P.; Vasková, Z.; Valigura, D.; Koman, M. *Acta Crystrallogr., Sect. E: Struct. Rep. Online* **2006**, *E62*, m109–m110.
(17) Lah, N.; Leban, I.; Clérac, R. *Eur. J. Inorg. Chem.* **2006**, 4888–4894.
(18) Lavalette, A.; Tuna, F.; Clarkson, G.; Alcock, N. W.; Hannon, M. J. *Chem. Commun.* **2003**, 2666–2667.
(19) Telfer, S. G.; Parker, N. D.; Kuroda, R.; Harada, T.; Lefebvre, J.; Leznoff, D. B. *Inorg. Chem.* **2008**, *47*(1), 209–218.
(20) Moncol, J.; Mudra, M.; Lönnecke, P.; Koman, M.; Melnik, M. *J. Coord. Chem.* **2004**, *57*(12), 1065–1078.
(21) Gupta, A. K.; Kim, J. *Acta Crystallogr., Sect. C: Cryst. Struct. Commun.* **2003**, *C59*, m262–m264.
(22) Ruben, M.; Breuning, E.; Barboiu, M.; Gisselbrecht, J.-P.; Lehn, J.-M. *Chem.—Eur. J.* **2003**, *9*(1), 291–299.
(23) Cao, X.-Y.; Harrowfield, J.; Nitschke, J.; Ramirez, J.; Stadler, A.-M.; Kyritsakas-Gruber, N.; Madalan, A.; Rissanen, K.; Russo, L.; Vaughan, G.; Lehn, J.-M. *Eur. J. Inorg. Chem.* **2007**, 2944–2965.
(24) Tielmann, P.; Marchal, A.; Lehn, J.-M. *Tetrahedron Lett.* **2005**, *46*, 6349–6353.
(25) Breuning, E.; Ziener, U.; Lehn, J.-M.; Wegelius, E.; Rissanen, K. *Eur. J. Inorg. Chem.* **2001**, 1515–1521.
(26) Ruben, M.; Ziener, U.; Lehn, J.-M.; Ksenofontov, V.; Gütlich, P.; Vaughan, G. B. M. *Chem.—Eur. J.* **2005**, *11*, 94–100.
(27) Hutchinson, D. J.; Hanton, L. R.; Moratti, S. C. *Acta Crystallogr., Sect. E: Struct. Rep. Online* **2009**, *E65*(7), o1546.

HSQC, gHMBC) spectra were collected on a 500 MHz Varian UNITY INOVA spectrometer at 298 or 348 K. Spectra were collected in $CDCl_3$ or d_6-DMSO and were referenced to the internal solvent signal. Chemical shifts are reported in δ units (ppm). Electrospray Mass Spectrometry (ESMS) was carried out on a Bruker microTOFQ instrument (Bruker Daltronics, Bremen, Germany). Samples were introduced using direct infusion into an ESI source in the positive mode. Sampling was averaged for 2 min over a m/z range of 50 to 3000 amu. The mass was calibrated using an external calibrant of sodium formate clusters, 15 calibrations points from 90 to 1050 amu, using a quadratic plus HPC line fit. ESMS spectra were processed using the Compass software (version 1.3, Bruker Daltronics, Bremen, Germany). UV−vis spectra were recorded on an Agilent 8453 spectrophotometer against a CH_3CN background using quartz cells with a 1 cm path length. Infrared (IR) spectra were recorded on a Perkin-Elmer Spectrum BX FT-IR system using KBr discs.

Caution! *Although no problems were encountered in this work, transition metal perchlorates are potentially explosive. They should be prepared in small amounts and handled with care.*

Syntheses. 6-Hydroxymethylpyridine-2-carboxaldehyde(2-methyl-pyrimidine-4,6-diyl)bis(1-methylhydrazone) (1). A solution of **2** (1.002 g, 5.50 mmol) and 6-hydroxymethyl-2-pyridinecarboxaldehyde (**3**) (1.627 g, 11.9 mmol) in EtOH (100 mL) was refluxed for 5 h under an inert atmosphere of N_2. Over the course of the reaction, a white solid precipitated out of the reaction solution. The reaction mixture was filtered, and the solid was washed with EtOH and dried *in vacuo* to give **1** as a white solid (2.138 g, 92%). Mp: 268−270 °C (decomp.). Anal. Found: C, 60.04; H, 5.71; N, 26.40. Calcd for $C_{21}H_{24}N_8O_2$: C, 59.99; H, 5.75; N, 26.64. ^{1}H NMR (500 MHz, DMSO-d_6), δ/ppm: 7.96 (2H, t, J = 7.7 Hz, H12), 7.88 (2H, d, J = 7.2 Hz, H11), 7.87 (2H, s, H9), 7.65 (1H, s, H5), 7.28 (2H, d, J = 7.5 Hz, H13), 5.37 (2H, t, J = 5.8 Hz, O*H*), 4.63 (4H, d, J = 5.8 Hz, H15), 3.65 (6H, s, H8), 2.47 (3H, s, H7). ^{13}C NMR (500 MHz, DMSO-d_6), δ/ppm: 165.44 (C2), 162.45 (C4, C6), 161.75 (C14), 153.21 (C10), 137.41 (C9), 136.87 (C12), 119.57 (C13), 116.92 (C11), 84.74 (C5), 64.06 (C15), 29.30 (C8), 25.79 (C7). ESMS m/z Found: 421.2134, 443.1929. Calcd for $C_{21}H_{25}N_8O_2^+$: 421.2095. Calcd for $C_{21}H_{24}N_8O_2Na^+$: 443.1914. Selected IR (KBr) ν/cm^{-1}: 3366 (m, br), 3236 (m, br, OH str), 2919 (m, C−H str), 1592 (s), 1561 (s, C═N str), 1489 (s), 1453 (s), 1412 (m), 1395 (s), 1265 (m), 1212 (m), 1165 (s), 1095 (m), 1038 (s). Crystals suitable for X-ray determination were grown from a DMSO solution of **1**.

Preparation of 6-Hydroxymethyl-2-pyridinecarboxaldehyde (3). The following method was modified from Artali et al.[28] MnO_2 (15.94 g, 183 mmol) was added slowly to a stirring solution of 2,6-bis(hydroxymethyl)pyridine (10.12 g, 72.7 mmol) in $CHCl_3$ (200 mL). The mixture was stirred and refluxed for 3 h, at which point more MnO_2 (12.71 g, 146 mmol) was added, and the reflux resumed for a further 3 h. After cooling, the mixture was filtered through Celite, and the black inorganic salts were washed with CH_3OH. The combined filtrate and washings were concentrated by rotary evaporation and the resulting oily residue subjected to column chromatography with an ethyl acetate/petroleum ether gradient (30 to 70%), giving the product as a white solid (5.049 g, 51%). Mp: 68−70 °C (lit. 66−69 °C[29]) Anal. Found: C, 60.59; H, 5.23; N, 10.07. Calcd for $C_7H_7NO_2$: C, 61.31; H, 5.14; N, 10.21. ^{1}H NMR (500 MHz, $CDCl_3$), δ/ppm: 10.09 (1H, s, C*H*O), 7.88 (2H, m, $H3_{py}$, $H5_{py}$), 7.52 (1H, m, $H4_{py}$), 4.88 (2H, s, CH_2). Selected IR (KBr), ν/cm^{-1}: 3134 (s, br, O−H str), 2847 (m, C−H str), 2718 (m, C−H str), 1712 (s, C═O str), 1601 (s), 1580 (m), 1450 (s), 1338 (s), 1317 (s), 1211 (m), 1114 (s), 1048 (s), 1001 (s).

Complexes. $Cu_2$1$(ClO_4)_4$. $Cu(ClO_4)_2\cdot 6H_2O$ (40.0 mg, 0.108 mmol) was dissolved in CH_3CN (2 mL) and added to **1** (21.8 mg, 0.052 mmol), resulting in the partial dissolution of **1** and the formation of a green solution. This mixture was stirred and heated until all the solid had dissolved. Diethyl ether was slowly diffused into this solution, resulting in the formation of green crystals. These crystals were filtered and dried *in vacuo* to yield Cu_2**1**$(ClO_4)_4$ as a green solid (15.7 mg, 32%). Anal. Found: C, 26.00; H, 3.04; N, 11.13. Calcd for $C_{21}H_{24}N_8O_{18}Cl_4Cu_2\cdot 2H_2O$: C, 25.70; H, 2.88; N, 11.42. ESMS m/z Found: 443.1894. Calcd for $C_{21}H_{24}N_8O_2Na^+$: 443.1914. UV−vis (CH_3CN), $\lambda_{max}(\varepsilon)$/nm (L mol^{-1} cm^{-1}): 691 (251). Selected IR (KBr), ν/cm^{-1}: 3455 (m, br, O−H str), 3062 (w, C−H str), 1630 (s), 1604 (s), 1589 (s), 1561 (s), 1498 (m), 1431 (m), 1386 (w), 1292 (m, C−O str), 1273 (m), 1158 (s), 1092 (s, br). Green crystals suitable for X-ray determination were grown by slow diffusion of diethyl ether into a CH_3CN solution of Cu_2**1**$(ClO_4)_4$.

$Cu_2$1$(SO_3CF_3)_4$. Cu_2**1**$(SO_3CF_3)_4$ was prepared as described for Cu_2**1**$(ClO_4)_4$ but using $Cu(SO_3CF_3)_2\cdot 4H_2O$ (31.0 mg, 0.0715 mmol) and **1** (10.7 mg, 0.0254 mmol) in CH_3CN (2 mL), which gave a green solution from which green crystals were obtained (26.2 mg, 90%). Anal. Found: C, 25.99; H, 2.39; N, 9.99. Calcd for $C_{25}H_{24}N_8O_{14}F_{12}S_4Cu_2$: C, 26.25; H, 2.11; N, 9.80. ESMS m/z Found: 482.1214, 844.9536, 994.9112. Calcd for $C_{21}H_{23}N_8O_2Cu^+$: 482.1234. Calcd for $C_{21}H_{23}N_8O_2Cu_2(SO_3CF_3)_2^+$: 844.9576. Calcd for $C_{21}H_{24}N_8O_2Cu_2(SO_3CF_3)_3^+$: 994.9153. UV−vis ($CH_3CN$), $\lambda_{max}(\varepsilon)$/nm(L mol^{-1} cm^{-1}): 699 (222). Selected IR (KBr), ν/cm^{-1}: 3445 (m, br, OH str), 3129 (w, CH str), 3061 (w, CH str), 1636 (m), 1622 (m,), 1603 (s), 1586 (s), 1558 (s), 1502(w), 1459 (w), 1428 (w), 1386 (w), 1260 (s, C−O str), 1177 (s), 1155 (s), 1059 (m), 1032 (s). Green crystals suitable for X-ray determination were grown by slow diffusion of diethyl ether into a CH_3CN solution of Cu_2**1**$(SO_3CF_3)_4$.

Cu(1H)$(ClO_4)_3$. Cu(**1**H)$(ClO_4)_3$ was prepared as described for Cu_2**1**$(ClO_4)_4$ but using $Cu(ClO_4)_2\cdot 6H_2O$ (73.0 mg, 0.197 mmol) and **1** (62.2 mg, 0.148 mmol) in CH_3CN (10 mL), which gave a green solution from which green crystals were obtained (87.1 mg, 75%). Anal. Found: C, 32.20; H, 3.22; N, 14.30. Calcd for $C_{21}H_{25}N_8O_{14}Cl_3Cu\cdot 0.5CH_3CN$: C, 32.87; H, 3.32; N, 14.81. ESMS m/z Found: 482.1245. Calcd for $C_{21}H_{23}N_8O_2Cu^+$: 482.1234. UV−vis (CH_3CN), $\lambda_{max}(\varepsilon)$/nm (L mol^{-1} cm^{-1}): 657 (171). Selected IR (KBr), ν/cm^{-1}: 3462 (m, br, O−H str), 3068 (m, CH str), 2931 (m, CH str), 1653 (m), 1616 (m), 1598 (s), 1558 (s), 1485 (m), 1455 (m), 1432 (m), 1406 (m), 1302 (m, C−O str), 1163 (m), 1089 (s, br), 1057 (s). Green crystals of differing morphology suitable for X-ray determination were grown by slow diffusion of diethyl ether into a CH_3CN solution of Cu(**1**H)$(ClO_4)_2$.

Cu1$(SO_3CF_3)_2$. Cu**1**$(SO_3CF_3)_2$ was prepared as described for Cu_2**1**$(ClO_4)_4$ but using $Cu(SO_3CF_3)_2\cdot 4H_2O$ (21.1 mg, 0.0486 mmol) and **1** (18.4 mg, 0.0437 mmol) in CH_3CN (4 mL), which gave a green solution from which green crystals were obtained (7.80 mg, 22%). Anal. Found: C, 34.52; H, 3.22; N, 13.89. Calcd for $C_{23}H_{24}N_8O_8F_6S_2Cu\cdot H_2O$: C, 34.52; H, 3.28; N, 14.00. ESMS m/z Found: 482.1199. Calcd for $C_{21}H_{23}N_8O_2Cu^+$: 482.1234. UV−vis (CH_3CN) $\lambda_{max}(\varepsilon)$/nm (L mol^{-1} cm^{-1}): 679 (170). Selected IR (KBr) ν/cm^{-1}: 3364 (m, br, OH str), 3055 (w, CH str), 1615 (m), 1597 (s), 1567 (s), 1547 (s), 1494 (m), 1461 (m), 1461 (m), 1424 (m), 1398 (m), 1364 (w), 1274 (s), 1249 (s), 1169 (m), 1116 (m), 1053 (m), 1030 (s). Green crystals suitable for X-ray determination were grown by slow diffusion of diethyl ether into a CH_3CN solution of Cu**1**$(SO_3CF_3)_2$.

X-Ray Crystallography. Details of the crystallographic data collection and refinement parameters are given in Table 1. X-ray diffraction data were collected on a Bruker APEX II CCD diffractometer, with graphite monochromated Mo Kα (λ = 0.71073 Å) radiation at 90 K in a nitrogen gas stream. Intensities

(28) Artali, R.; Botta, M.; Cavallotti, C.; Giovenzana, G. B.; Palmisano, G.; Sisti, M. *Org. Biomol. Chem.* **2007**, *5*, 2441–2447.

(29) Okuyama, Y.; Nakano, K.; Kabuto, C.; Nozawa, E.; Takahashiu, K.; Hongo, H. *Heterocycles* **2002**, *58*, 457–460.

Table 1. Crystallographic Data

	1	$[Cu_2\mathbf{1}(CH_3CN)_4](ClO_4)\cdot CH_3CN$ (**4**)	$[Cu_2\mathbf{1}(SO_3CF_3)_2(CH_3CN)_2](SO_3CF_3)_2\cdot CH_3CN$ (**5**)	$[Cu(\mathbf{1}H)(ClO_4)_2](ClO_4)$ (**6**)
formula	$C_{21}H_{24}N_8O_2$	$C_{31}H_{39}Cl_4Cu_2N_{13}O_{18}$	$C_{31}H_{33}Cu_2F_{12}N_{11}O_{14}S_4$	$C_{21}H_{25}Cl_3CuN_8O_{14}$
fw	420.48	1150.63	1267.00	783.38
cryst syst	triclinic	triclinic	triclinic	monoclinic
space group	$P\bar{1}$	$P\bar{1}$	$P\bar{1}$	$P2(1)/c$
a/Å	7.2289(17)	10.4995(7)	13.1415(19)	11.1743(9)
b/Å	10.044(2)	13.3286(8)	13.909(2)	12.5567(11)
c/Å	15.247(4)	17.5470(11)	15.291(3)	20.6999(19)
α/deg	96.133(12)	80.749(3)	96.715(7)	90.000
β/deg	96.304(13)	76.047(4)	106.583(7)	102.655(4)
γ/deg	108.676(13)	78.554(3)	115.590(7)	90.000
V/Å^3	1030.5(4)	2319.2(3)	2320.9(7)	2833.7(4)
Z	2	2	2	4
T/K	90(2)	90(2)	90(2)	90(2)
μ/mm^{-1}	0.093	1.233	1.220	1.141
reflns collected	10055	21557	27415	37579
unique reflns (R_{int})	3830 (0.0276)	8147 (0.0407)	7996 (0.0405)	4976 (0.0348)
R_1 indices [$I > 2\sigma(I)$]	0.0535	0.0614	0.0604	0.0318
wR_2 (all data)	0.1850	0.1513	0.1714	0.0796
goodness-of-fit	1.027	1.043	1.065	1.078

	$[Cu(\mathbf{1}H)(CH_3CN)](ClO_4)_3\cdot 0.5H_2O$ (**7**)	$[Cu\mathbf{1}(SO_3CF_3)]_2(SO_3CF_3)_2\cdot CH_3CN$ (**8**)
formula	$C_{23}H_{28}Cl_3CuN_9O_{14.50}$	$C_{48}H_{49}Cu_2F_{12}N_{17}O_{16}S_4$
fw	832.43	1603.36
cryst syst	triclinic	triclinic
space group	$P\bar{1}$	$P\bar{1}$
a/Å	9.5283(13)	14.2625(9)
b/Å	11.2257(15)	16.2630(11)
c/Å	16.279(3)	16.7874(12)
α/deg	79.320(9)	104.770(4)
β/deg	84.008(10)	103.449(5)
γ/deg	73.075(8)	94.037(4)
V/Å^3	1634.6(5)	3627.0(4)
Z	2	2
T/K	90(2)	90(2)
μ/mm^{-1}	0.996	0.802
reflns collected	22579	22581
unique reflns (R_{int})	5987 (0.0429)	10641 (0.0346)
R_1 indices [$I > 2\sigma(I)$]	0.0480	0.0807
wR_2 (all data)	0.1417	0.1951
goodness-of-fit	1.044	1.99

were corrected for Lorentz polarization effects,[30] and a multiscan absorption correction[31] was applied. The structures were solved by direct methods (SHELXS[32] or SIR-97[33]) and refined on F^2 using all data by full-matrix least-squares procedures (SHELXL 97[34]). All calculations were performed using the WinGX interface.[35] Detailed analyses of the extended structure were carried out using PLATON[36] and MERCURY[37] (version 1.4.1). X-ray data were deposited with the Cambridge Crystallographic Data Center CCDC-773524−CCDC-773529. These data can be obtained free of charge from the Cambridge Crystallographic Data Center via www.ccdc.cam.ac.uk/data_request/cif.

Some of the crystal structures contained disordered components. One of the ClO_4^- counterions in $[Cu_2\mathbf{1}(CH_3CN)_4](ClO_4)_4\cdot CH_3CN$ (**4**) showed translational disorder over two sites, with site occupancy factors of 0.68 and 0.32. One of the coordinated ClO_4^- ions in $[Cu(\mathbf{1}H)(ClO_4)_2](ClO_4)$ (**6**) showed rotational disorder about a 3-fold axis with site occupancy factors of 0.83 and 0.17. One of the ClO_4^- counterions in $[Cu(\mathbf{1}H)(CH_3CN)](ClO_4)_3\cdot 0.5H_2O$ (**7**) showed translational disorder over two sites with site occupancy factors of 0.50 and 0.50. Complex **7** also contained a H_2O molecule that was only present half the time. The H atoms on this H_2O molecule were not located. One of the $SO_3CF_3^-$ counterions in $[Cu\mathbf{1}(SO_3CF_3)]_2(SO_3CF_3)_2\cdot CH_3CN$ (**8**) was disordered over two sites with site occupancy factors of 0.66 and 0.34. The ADP values and bond distances seen in both parts of the disordered $SO_3CF_3^-$ counterion were restrained using the EADP and DFIX commands, respectively. Additionally, there appeared to be a chain of disordered CH_3CN molecules in **8** which could not be modeled. The SQUEEZE option of PLATON[36] was therefore employed to remove them from the structure. The number of electrons located was 101 per unit cell, and this was assigned to 4.5 CH_3CN molecules of solvent.

Results and Discussion

The ligand (**1**) was designed with terminal hydroxymethyl groups so that it could be incorporated into a larger molecular structure. The 4,6-bis(1-methylhydrazino)pyrimidine

(30) *SAINT Software Reference Manual*; Bruker AXS: Madison; WI, 1998.
(31) Sheldrick, G. M. *SADABS, Program for Absorption Correction*; University of Göttingen: Göttingen, Germany, 1996.
(32) Sheldrick, G. M. *Acta Crystallogr., Sect. A: Found. Crystallogr.* **1990**, *A46*(6), 467–473.
(33) Altomare, A.; Burla, M. C.; Camalli, M.; Cascarano, G. L.; Giacovazzo, C.; Guagliardi, A.; Moliterni, A. G. G.; Polidori, G.; Spagna, R. *J. Appl. Crystallogr.* **1999**, *32*, 115–119.
(34) Sheldrick, G. M. *SHELXL−97, Program for the Solution of Crystal Structures*; University of Göttingen: Göttingen, Germany, 1997.
(35) Farrugia, L. J. *J. Appl. Crystallogr.* **1999**, *32*, 837–838.
(36) Spek, A. L. *Acta Crystallogr., Sect A: Found. Crystallogr.* **1990**, *46*, C34.
(37) (a) Macrae, C. F.; Edgington, P. R.; McCabe, P.; Pidcock, E.; Shields, G. P.; Taylor, R.; Towler, M.; van de Streek, J. *J. Appl. Crystallogr.* **2006**, *39*, 453–457. (b) Bruno, I. J.; Cole, J. C.; Edgington, P. R.; Kessler, M. K.; Macrae, C. F.; McCabe, P.; Pearson, J.; Taylor, R. *Acta Crystallogr., Sect. B: Struct. Sci.* **2002**, *B58*, 389–397.

Scheme 1.[a]

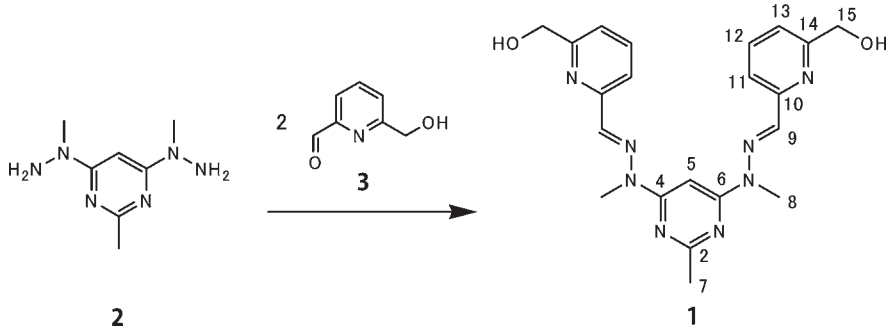

[a] Showing NMR numbering.

precursor (**2**) was prepared by the treatment of 4,6-dichloro-2-methylpyrimidine with methyl hydrazine.[4] The structure of **2** in solution and in the solid state has been described elsewhere.[27] The arm component, 6-hydroxymethyl-2-pyridinecarboxaldehyde (**3**), was synthesized through activated MnO_2 oxidation of one of the alcohol groups of commercially available 2,6-bis(hydroxymethyl)pyridine.[28] Chromatography with silica gel (10% hydrated v/v) and a gradient of ethyl acetate/petroleum ether (30 to 70%) as the eluant was found to be the most efficient means of purifying **3**. It was also discovered that any unreacted 2,6-bis(hydroxymethyl)-pyridine could be recovered from the chromatography column by eluting it with iso-propanol.

Synthesis and Structure of 1. Ligand **1** was produced in high yield by a condensation reaction of **2** and **3** in a 1:2 molar ratio (Scheme 1). No workup was needed as **1** precipitated out of the solution as a pure white solid. The ligand was found to be only sparingly soluble in pyridine, $CHCl_3$, DMSO, and DMF at 50 °C. ^{1}H and ^{13}C NMR spectra of **1** were collected from a dilute DMSO-d_6 solution at elevated temperatures. The ^{1}H NOE correlation between the proton of the pyrimidine ring (H5) and the H11 protons of the terminal pyridine rings, combined with the lack of any correlation between the methyl protons on the ternary N_{hyz} atom (H8) and H5, showed that **1** adopted a folded shape in solution, with both the pym−hyz bonds in a *transoid* conformation (Scheme 1). The IR spectrum showed a broad peak at 3236 cm^{-1}, corresponding to the OH stretching mode, and a strong peak at 1561 cm^{-1}, which was attributed to the stretching mode of the newly formed imine bond. The ESMS spectrum showed a base peak at m/z 421.2134 corresponding to the molecular ion $[\mathbf{1} + H]^+$. The microanalysis results were consistent with the predicted formula for **1**.

X-Ray Structure of $C_{21}H_{24}N_8O_2$, 1. The low solubility of **1** in most organic solvents made obtaining X-ray-quality crystals difficult. Crystals of suitable quality were eventually obtained from a dilute DMSO solution of **1** which was left standing for over two months. Ligand **1** crystallized in the triclinic space group $P\bar{1}$. The asymmetric unit contained one complete ligand molecule folded in a horseshoe conformation, with both pym−hyz bonds ($C9_{pym}$−$N3_{hyz}$ and $C11_{pym}$−$N6_{hyz}$) in a *transoid* conformation (Figure 2). The distance across the horseshoe, from the centroid of one of the terminal pyridine rings to the other, was 6.73 Å. The three methyl groups (C8, C13, and C14) and $N1_{py}$ and $N8_{py}$ atoms were arranged on the outside of the horseshoe, while the ternary N_{hyz} atoms ($N2_{hyz}$ and $N7_{hyz}$) pointed inward. Conjugation between the pyrimidine ring and hydrazone bonds resulted in the majority of **1** lying in the mean plane of the central pyrimidine ring (C9, C10, C11, C12, N4, N5). The terminal pyridine rings were twisted with respect to this plane in such a way that both the $N1_{py}$ and $N8_{py}$ (py = pyridine) atoms occupied the same side of the mean plane. The angles between the mean plane and the plane of the $N1_{py}$ and $N8_{py}$ containing pyridine rings were 7.74° and 8.04°, respectively. The hydroxymethyl arm on the pyridine ring containing $N1_{py}$ lay in the mean plane, while the corresponding group on the pyridine ring containing $N8_{py}$ was twisted out of this plane by 83.76°.

Molecules of **1** were organized into centrosymmetic-stepped dimers through self-complementary H-bonding interactions between the hydroxymethyl arms (Figure 2). The O1−H···O2A distance was 1.970(2) Å (corresponding to an O1···O2A separation of 2.707(2) Å). This arrangement of the two horseshoe ligands created a shape which was reminiscent of a macrocycle. These cyclic dimers were linked together through self-complementary H-bonding between O2−H···N8B at a distance of 1.901(2) Å [corresponding to an O2···N8B separation of 2.720(2) Å], which formed a 1D chain in the diagonal [1 1 0] direction. These chains were arranged into a 2D sheet through two types of $\pi-\pi$ stacking interactions involving alternating pyridine rings [centroid-to-centroid distances: $N8_{py}$···$N8_{py}$ = 3.7065(15) and $N8_{py}$···$N1_{py}$ = 3.8682(15) Å]. An additional π-stacking interaction between interdigitated pyrimidine rings of adjacent sheets extended the structure into three dimensions [centroid-to-centroid distance: 3.7277(14) Å].

Synthesis and Structures of Complexes. The Cu(II) salts, $Cu(ClO_4)_2 \cdot 6H_2O$ or $Cu(CF_3SO_3)_2 \cdot 4H_2O$, were dissolved in CH_3CN and added to **1** in either a 2:1 or 1:1 molar ratio. While **1** was not soluble in CH_3CN, the addition of the metal salt, with agitation and heat, resulted in dissolution of **1** upon complexation to form a clear green solution of the desired complex. UV−vis spectroscopy was performed on these solutions; thereafter the complexes were crystallized by the slow diffusion of diethyl ether. These crystals were used for single-crystal X-ray analysis. Additional solid material was produced in a similar fashion and was filtered and dried *in vacuo*, then analyzed by microanalysis, ESMS, and IR spectroscopy.

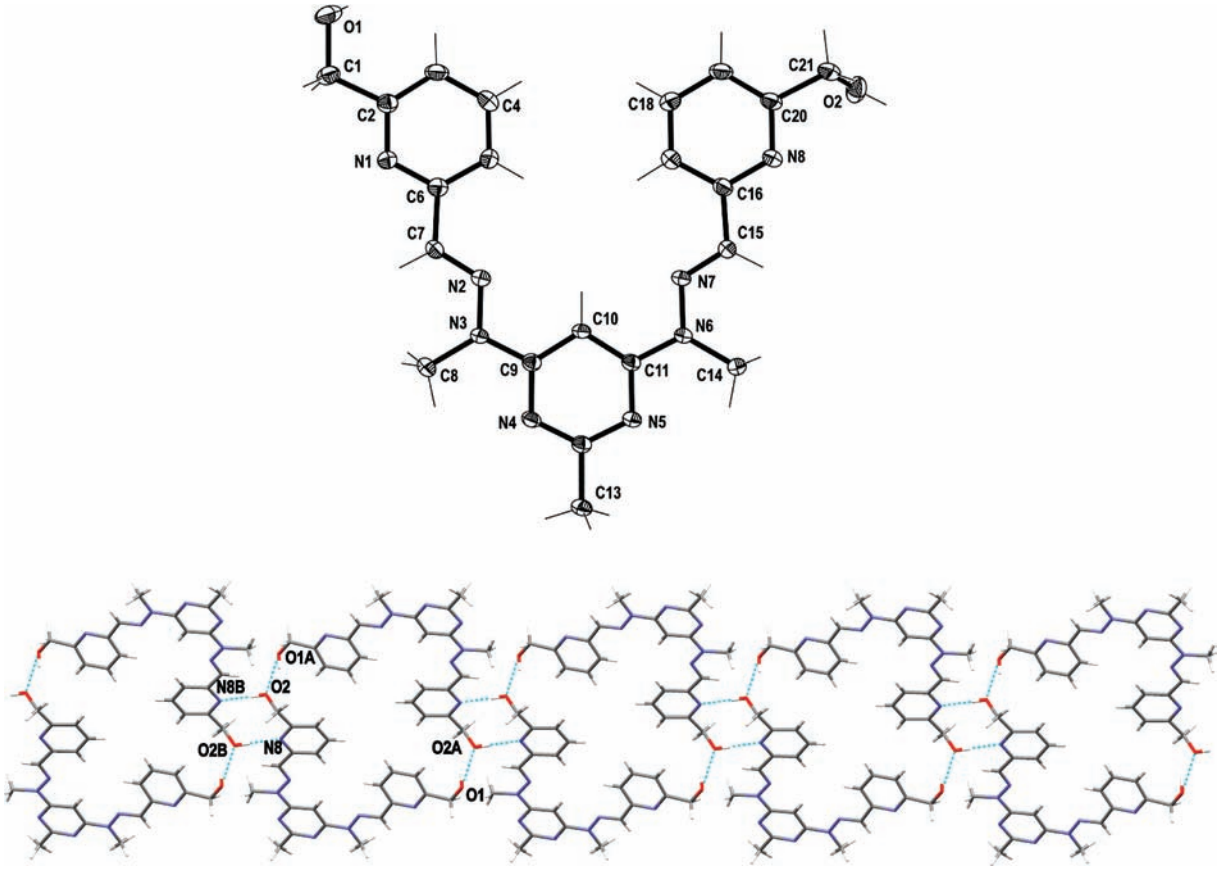

Figure 2. (Top) View of **1** (crystallographic numbering). Thermal ellipsoids drawn at the 50% probability level. (Bottom) View showing the assembly of **1** into a 1D chain of dimers, along the [1 1 0] direction, through H-bonding (symmetry codes, A: $2 - x$, $1 - y$, $2 - z$; B: $1 + x$, $-1 + y$, z).

$Cu_2$1$(ClO_4)_4$. The UV−vis spectrum of the solution showed a single broad peak at 691 nm. The microanalytical result of the dried crystals was consistent with the formula Cu_2**1**$(ClO_4)_4 \cdot 2H_2O$. The complex fragmented and lost Cu(II) ions during ESMS, resulting in a base peak at m/z 443.18942 which was consistent with the ion $[\mathbf{1} + Na]^+$. IR spectroscopy showed that coordination of the Cu(II) ions increased the frequency of the OH stretching mode to 3455 cm^{-1}. Four of the pym and py stretching modes and the C═N stretching mode occurred between 1630 and 1561 cm^{-1}.

X-Ray Structure of $[Cu_2$1$(CH_3CN)_4](ClO_4)_4 \cdot CH_3CN$, 4. Complex **4** crystallized in the triclinic space group $P\bar{1}$, with one $[Cu_2$**1**$(CH_3CN)_4]^{4+}$ cation, four ClO_4^- counterions, and a CH_3CN of crystallization in the asymmetric unit. The complex had a slightly bowed linear shape, with both pym−hyz linkages in a *cisoid* conformation. The centroid-to-centroid distance between the terminal pyridine rings of **4** was 12.59 Å, which was almost twice the length measured in the free ligand. A Cu(II) ion was bound to each of the pym−hyz−py coordination sites. The Cu1 ion was bound to the three N donors, and the hydroxymethyl O donor of the pym−hyz−py coordination site, while Cu2 was only bound to the three N donors of the pym−hyz−py coordination site, and not to the hydroxymethyl O donor. The coordination sphere of each Cu(II) ion was completed by two CH_3CN molecules. Cu1 had a six coordinate, tetragonally distorted octahedral geometry, with elongated Cu−N bonds to the out-of-plane CH_3CN ligands.[38] Cu2 was present in a five coordinate environment with a τ_5 parameter of 0.605, which was consistent with a distorted trigonal bipyramid geometry.[39] The axial sites were occupied by the $N5_{pym}$ and $N8_{py}$ donors, while the two CH_3CN molecules and the $N7_{hyz}$ donor occupied the three equatorial sites (Figure 3).

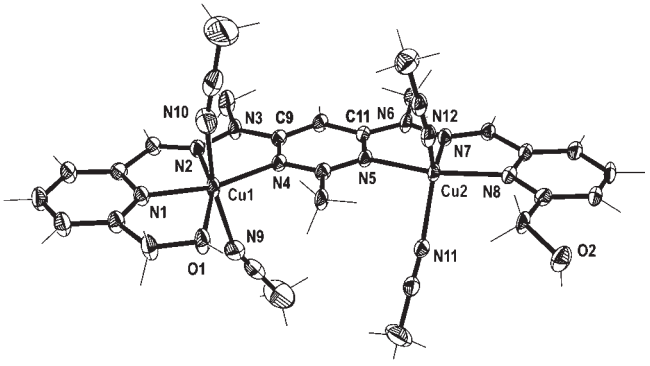

Figure 3. View of the $[Cu_2$**1**$(CH_3CN)_4]^{4+}$ cation showing the coordination environments about the Cu(II) ions (crystallographic numbering). Thermal ellipsoids drawn at the 50% probability level.

The distance from the Cu(II) ions and the mean plane through the central pyrimidine ring (C9, C10, C11, C12, N4, N5) was 0.193 Å for Cu1 and 0.064 Å for Cu2,

(38) Hathaway, B. J. *Comprehensive Coordination Chemistry*; Pergamon: Oxford, U. K., 1987; Vol. 5.

(39) Addison, A. W.; Rao, T. N.; Reedijk, J.; van Rijn, J.; Verschoor, G. C. *J. Chem. Soc., Dalton Trans.* **1984**, 7, 1349–1356.

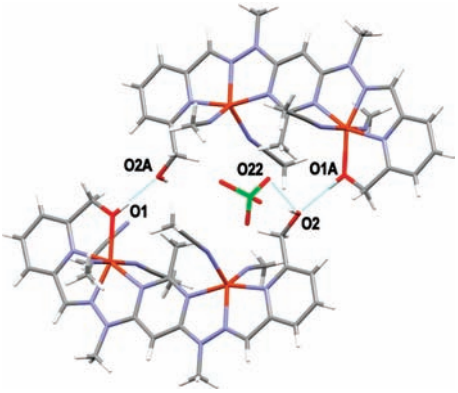

Figure 4. View of two $[Cu_2\mathbf{1}(CH_3CN)]^{4+}$ cations arranged into an offset dimer through H-bonding interactions. The ClO_4^- counteranion H-bonded to O2 is also shown (symmetry codes, A: $1-x$, $1-y$, $1-z$).

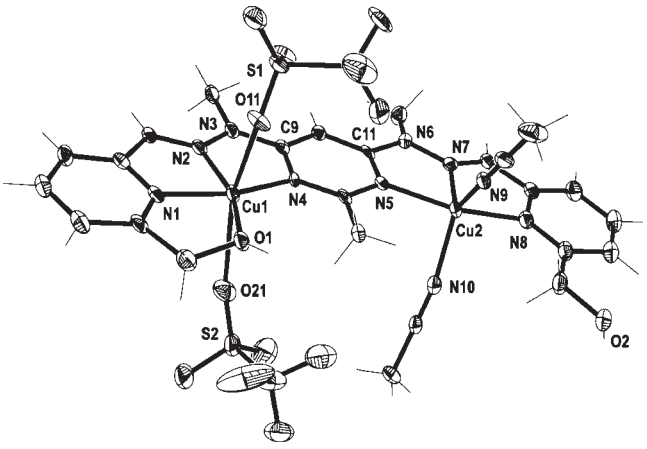

Figure 5. View of the $[Cu_2\mathbf{1}(SO_3CF_3)_2(CH_3CN)_2]^{2+}$ cation showing the coordination environment about the Cu(II) ions (crystallographic numbering). Thermal ellipsoids drawn at the 50% probability level.

respectively. The complex was slightly bowed out of the mean plane, such that the terminal pyridine rings both resided on the same side of the mean plane as the two Cu(II) ions. The angle between the plane of the pyridine ring containing N1 and the mean plane was 4.77°, while for the pyridine ring containing N8, this angle was 4.56°.

The complex was arranged into discrete offset dimers by self-complementary H-bonding between O1 and O2 of the hydroxymethyl arms (Figure 4). The O1−H···O2A distance was 1.844(3) Å [corresponding to an O1···O2A distance of 2.633(5) Å]. Additionally, one of the free ClO_4^- anions was weakly H-bonded to O2 with an O2−H···O22 distance of 2.425(8) Å [corresponding to an O2···O22 distance of 3.125(9) Å].

$Cu_2\mathbf{1}(SO_3CF_3)_4$. The UV−vis spectrum showed a single broad peak at 699 nm. Dark green crystals were grown by the slow diffusion of diethyl ether into a CH_3CN solution of the complex. The microanalytical results for the dried crystals were consistent with the complex formula $Cu_2\mathbf{1}(SO_3CF_3)_4$. ESMS showed peaks at m/z 844.9536 and 944.9112, which were assigned to the molecular fragments $[Cu_2(\mathbf{1}\text{-H})(SO_3CF_3)_2]^+$ and $[Cu_2\mathbf{1}(SO_3CF_3)_3]^+$, respectively. The IR spectrum showed the OH stretching mode at 3445 cm^{-1}. There were five peaks between 1636 and 1558 cm^{-1}, due to the pym, py, and C=N stretching modes.

X-Ray Structure of $[Cu_2\mathbf{1}(SO_3CF_3)_2(CH_3CN)_2](SO_3CF_3)_2\cdot CH_3CN$, 5. Complex **5** crystallized in the triclinic space group $P\bar{1}$ with one $[Cu_2\mathbf{1}(SO_3CF_3)_2(CH_3CN)_2]^{2+}$ cation, two $SO_3CF_3^-$ counterions, and a CH_3CN of crystallization in the asymmetric unit. The ligand backbone had a slightly bowed linear shape, similar to complex **4**, with a length between the terminal pyridine ring centroids of 12.67 Å. Both pym−hyz bonds adopted a *cisoid* conformation, and there was a Cu(II) ion bound to each of the two pym−hyz−py coordination sites. Cu1 was present in an elongated tetragonal octahedral geometry[38] with the O1, $N1_{py}$, $N2_{hyz}$, and $N4_{pym}$ donors of the pym−hyz−py coordination pocket in equatorial positions and the O11 and O21 donors of two different $SO_3CF_3^-$ anions in axial positions. The Cu2 coordination sphere of **5** closely resembled that of Cu2 in **4**. Cu2 was present in a five coordinate distorted trigonal bipyramidal geometry with a τ_5 parameter of 0.574.[39] The $N5_{pym}$ and $N8_{py}$ donors were present in the axial sites, while the $N7_{hyz}$ donor and the N9 and N10 donors of the two bound CH_3CN molecules were bound in the equatorial positions. The O2 donor was not bound to Cu2 and was instead orientated away from Cu2 (Figure 5).

Most of the ligand backbone lay in the mean plane of the central pyrimidine ring. A slight twist to the complex meant that the $N1_{py}$ and $N8_{py}$ containing pyridine rings projected out from either side of the mean plane by angles of 3.53° and 4.57°, respectively. Cu1 and Cu2 sat above and below the mean plane through the central pyrimidine ring by 0.096 and 0.092 Å, respectively. The only noticeable intermolecular contact was a H bond between O2 and a symmetry generated $SO_3CF_3^-$ counterion. The O2−H···O41 distance was 2.482(4) Å [corresponding to a O2···O41 distance of 2.896(6) Å.

Cu(1H)$(ClO_4)_3$. The UV−vis spectrum showed a single broad peak at 657 nm. Dark green needle-shaped crystals were obtained by the slow diffusion of diethyl ether into this solution. Closer inspection revealed that there were two different morphologies of green crystals growing from the one solution. Single-crystal X-ray structural analysis was successfully performed on a crystal of each morphology, yielding the structural solutions [Cu(**1**H)-$(ClO_4)_2](ClO_4)$ (**6**) and $[Cu(\mathbf{1}H)(CH_3CN)](ClO_4)_3\cdot 0.5H_2O$ (**7**). The $N8_{py}$ donor was protonated in both isomers. The microanalytical result from additional solid material was consistent with the formula $Cu\mathbf{1}H(ClO_4)_3\cdot 0.5CH_3CN$. The ESMS spectrum of the dried material showed a peak at m/z 482.1245, corresponding to the ion fragment $C_{21}H_{23}$-$N_8O_2Cu^+$. The IR spectrum obtained showed the O−H stretching mode at 3462 cm^{-1} and four pym, py, and C=N stretching modes between 1653 and 1558 cm^{-1}.

X-Ray Structure of $[Cu(\mathbf{1}H)(ClO_4)_2](ClO_4)$, 6. Complex **6** crystallized in the monoclinic space group $P2_1/c$ with one $[Cu(\mathbf{1}H)(ClO_4)_2]^+$ cation and one ClO_4^- counterion in the asymmetric unit. The complex had an asymmetric bent shape, as the pym−hyz bond of the coordination pocket occupied with the Cu(II) ion ($C9_{pym}$−$N3_{hyz}$) had a *cisoid* arrangement, while the pym−hyz bond of the uncoordinated pym−hyz−py site ($C11_{pym}$−$N6_{hyz}$) maintained a *transoid* conformation. As a result, the O1 to $C9_{pym}$ half of the complex had a slightly bowed, linear shape reminiscent of complexes **4** and **5**, while the $C11_{pym}$ to O2 half of the complex had a half horseshoe shape

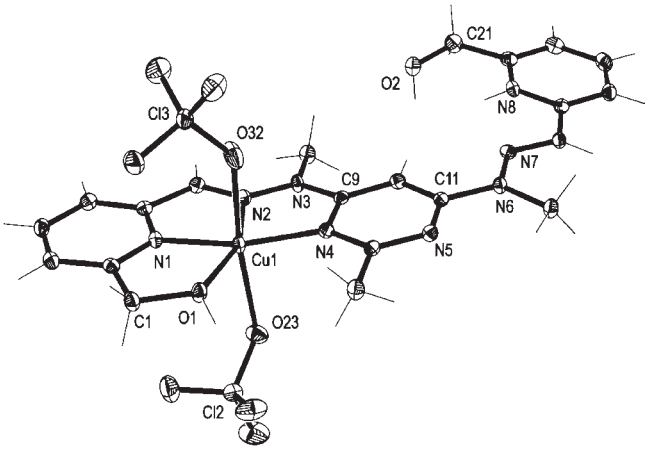

Figure 6. View of the $[Cu(1H)(ClO_4)_2]^+$ cation showing the coordination environment about the Cu(II) ion and the *cisoid* $N3_{hyz}-C9_{pym}$ and *transoid* $C11_{pym}-N6_{hyz}$ bonds (crystallographic numbering). Thermal ellipsoids drawn at the 50% probability level.

similar to that of the structure of uncoordinated **1** (Figure 6). The centroid-to-centroid distance between the terminal pyridine rings was 12.11 Å.

The Cu(II) ion adopted a tetragonally distorted octahedral geometry,[38] with the donors O1, $N1_{py}$, $N2_{hyz}$, and $N4_{pym}$ arranged in equatorial positions and the O23 and O32 donors from two different ClO_4^- anions in axial coordination sites (Figure 6). The Cu(II) ion was raised out of the mean plane of the central pyrimidine ring by 0.105 Å. The ligand backbone had a slight curve, such that the terminal pyridine rings pointed away from the mean plane of the central pyrimidine ring at angles of 5.88° for the $N1_{py}$ ring and 9.52° for the $N8_{py}$ ring. In addition, the $N8_{py}$ containing pyridine ring was tilted with respect to the rest of the molecule such that its plane intersected the mean plane of the central pyrimidine ring at an angle of 9.52°. The $N8_{py}$ and O2 donors were orientated toward the center of the vacant pym−hyz−py coordination pocket, and the $N8_{py}$ donor was protonated.

The resultant positive charge on $N8_{py}$ was balanced by a third ClO_4^- counterion which bridged neighboring $[Cu(1H)(ClO_4)_2]^+$ cations through H-bonding between O14 on the ClO_4^- counterion and the O1 and O2 terminal OH arms on the neighboring cations. The O1−H···O14 and O2A−H···O14 distances were 2.048(2) and 2.502(2) Å, respectively, [corresponding to O1···O14 and O2A···O14 distances of 2.799(2) and 2.819(3) Å, respectively]. In addition, an intramolecular H bond existed between O1 and O24 of the ClO_4^- bound to Cu1, with an O1−H···O24 distance of 2.474(2) Å [corresponding to an O1···O24 distance of 2.977(3) Å]. O2A was also H-bonded to O13 on the bridging ClO_4^- counterion, with an O2A−H···O13 distance of 2.819(3) Å [corresponding to an O2A···O13 distance of 3.289(2) Å]. Molecules of **6** were arranged through H-bonding with the bridging ClO_4^- counterion into propeller-shaped 1D chains, with an angle of 36.62° between the central pyrimidine mean planes of neighboring molecules (Figure 7). These chains ran along the *c* axis and were organized into pairs through self-complementary offset face-to-face $\pi-\pi$ stacking interactions, which existed between the central pyrimidine and the $N8_{py}$ containing pyridine rings [centroid-to-centroid distance of 3.697(2) Å]

X-Ray Structure of $[Cu(1H)(CH_3CN)](ClO_4)_3 \cdot 0.5H_2O$, 7. Complex **7** crystallized in the triclinic space group $P\bar{1}$ with one $[Cu(1H)(CH_3CN)]^{3+}$ cation, three ClO_4^- counterions, and a disordered H_2O of crystallization in the asymmetric unit. Complex **7** had a similar asymmetric bent shape to **6**. The Cu(II) ion in **7** was coordinated to the O1, $N1_{py}$, $N2_{py}$, and $N4_{pym}$ donors of one of the pym−hyz−py sites on **1**. It was also coordinated to a CH_3CN molecule, giving the Cu(II) ion a five-coordinate, pseudosquare pyramidal geometry, with a τ_5 parameter of 0.048.[39] The Cu(II) ion was raised slightly above the mean plane of the central pyrimidine ring by 0.108 Å. As in **6**, the coordination of the Cu(II) ion held the $N2_{hyz}-C9_{pym}$ bond in its *cisoid* conformation and gave the O1 to $C9_{pym}$ half of the ligand a slightly bowed, linear shape. This half of the ligand also curved away from the mean plane of the central pyrimidine ring such that the $N1_{py}$ containing pyridine ring resided at an angle of 4.32° above the mean plane. The $C11_{pym}-C21$ half of **7** closely resembled that of **6**. It had the same half horseshoe shape, and $N8_{py}$ was similarly orientated toward the middle of the molecule and was protonated. The plane of the $N8_{py}$ containing pyridine ring was tilted to a greater extent in **7** as its plane intersected the mean plane through the central pyrimidine ring at an angle of 17.34°. In contrast to **6**, the hydroxymethyl O2 donor in **7** pointed away from the vacant pym−hyz−py coordination pocket (Figure 8). The distance between the centroids of the terminal pyridine rings was 12.30 Å, which was slightly longer than that of **6**.

The hydrogen on N8 was involved in a bifurcated H bond with O24 on the ClO_4^- counterion, which sat above the vacant pym−hyz−py coordination pocket, and a disordered H_2O (O3) molecule, which resided below the empty pocket. The N8−H···O24 distance was 2.697(4) Å [corresponding to a N8···O24 distance of 3.064(5) Å], while the N8−H···O3 distance was 2.172(7) Å [corresponding to a N8···O3 distance of 2.949(8) Å]. That same ClO_4^- counterion was also H-bonded to O2A on a neighboring $[Cu(1H)(CH_3CN)]^{3+}$ cation through O23, with an O2A−H···O23 distance of 2.233(4) Å [corresponding to an O2A···O23 distance of 2.785(5) Å] (Figure 9). The ClO_4^- counterion containing Cl1 was held in an unusual position beneath the Cu1−O1 coordination bond by a H bond between O13 and O1−H and a weak interaction between O12 and Cu1 (Figure 9). The O1−H···O13 distance was 2.208(4) Å [corresponding to an O1···O13 distance of 2.662(5) Å], while the O12···Cu1 distance was 2.845(4) Å. A search of $O_3Cl-O-Cu(II)$ bond distances in the Cambridge Stuctural Database (CSD version 5.29)[40] revealed that this O12···Cu1 distance is above the upper quartile (2.73 Å) of all reported bond lengths (923 bond distances in 663 complexes, range from 1.91 to 3.58 Å). Therefore, the O12···Cu1 distance was too long to be considered a bond, but the unusual clamp-like positioning of the ClO_4^- counterion over the Cu1−O1 bond suggested some weak interaction was present between Cu1 and O12. The other ClO_4^- counterion, which contained Cl3, was

(40) Allen, F. H.; Davies, J. E.; Galloy, J. J.; Johnson, O.; Kennard, O.; Macrae, C. F.; Mitchell, E. M.; Mitchell, G. F.; Smith, J. M.; Watson, D. G. *J. Chem. Inf. Comput. Sci.* **1991**, *31*, 187–204.

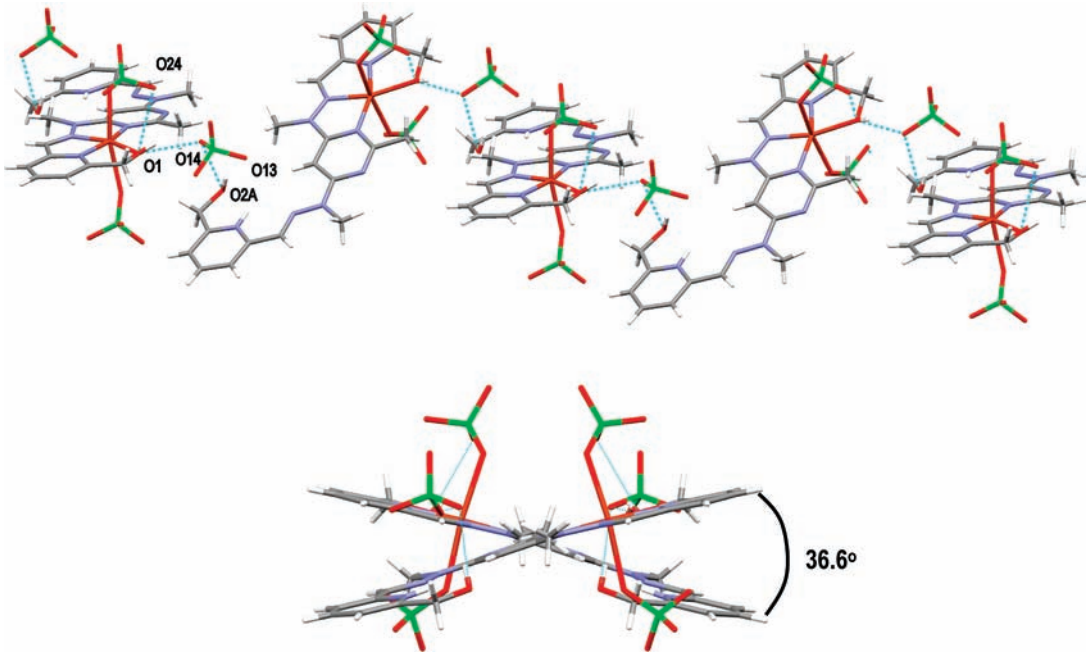

Figure 7. (Top) View of the arrangement of the $[Cu(\mathbf{1}H)(ClO_4)_2]^+$ cations into a 1D chain through bifurcated H-bonding between the hydroxymethyl groups (O1 and O2) on neighboring cations with the ClO_4^- counteranion (O13 and O14). The intramolecular H bond between O24 on the ClO_4^- anion bound to Cu1 and O1−H can be seen also (symmetry codes, A: x, $3/2 - y$, $1/2 + z$). (Bottom) View of the one-dimensional chain along the c direction showing the propeller shape created by the 36.62° angle between the planes of alternating cations.

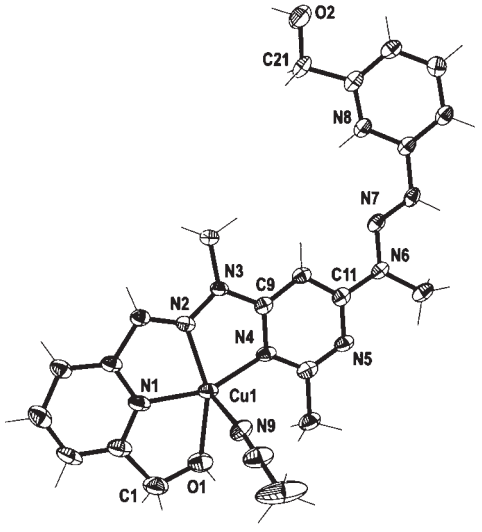

Figure 8. View of the $[Cu(\mathbf{1}H)(CH_3CN)]^{3+}$ cation showing the coordination environment about the Cu(II) ion and the *cisoid* $N3_{hyz}-C9_{pym}$ and *transoid* $C11_{pym}-N6_{hyz}$ bonds (crystallographic numbering). Thermal ellipsoids drawn at the 50% probability level.

disordered over two sites, so possible H bonds were not described.

Cu1(SO$_3$CF$_3$)$_2$. The UV−vis spectrum showed a single broad peak at 679 nm. Crystals were extremely hard to grow. After many attempts, a batch of single crystals suitable for X-ray determination were obtained through the slow diffusion of diethyl ether into the complex solution. The data from the first three X-ray experiments were not of high enough quality to yield a stable structural solution. For the fourth experiment, data were collected on the crystal over 48 h, and the structure (described below) was able to be refined successfully. Each of the four crystals used gave the same cell, space group, and structural solution. The microanalytical result of the dried crystals was consistent with the complex formula Cu**1**(SO$_3$CF$_3$)$_2$. The IR spectrum showed the OH stretching peak at 3364 cm^{-1}, and five peaks between 1615 and 1494 cm^{-1} due to various pym, py, and C=N stretching modes.

X-Ray Structure of [Cu1(SO$_3$CF$_3$)]$_2$(SO$_3$CF$_3$)$_2$·CH$_3$CN 8. Complex **8** crystallized in the triclinic space group $P\bar{1}$ with two $[Cu\mathbf{1}(SO_3CF_3)]^+$ cationic units, two $SO_3CF_3^-$ counterions, and a CH_3CN molecule of crystallization in the asymmetric unit. There were also 4.5 disordered CH_3CN molecules in the unit cell; however, these were removed from the structure with the SQUEEZE procedure, as they could not be modeled effectively. Both of the $[Cu\mathbf{1}(SO_3CF_3)]^+$ cations had a bent shape similar to that of complexes **6** and **7**, with one Cu(II) ion bound in one of the pym−hyz−py coordination pockets in each cation. As seen in **6** and **7**, the pym−hyz bond of the occupied coordination site adopted a *cisoid* conformation, while the pym−hyz bond of the unoccupied site maintained a *transoid* conformation. The two cations were stacked on top of each other in an off-center head-to-toe fashion. They were arranged almost parallel to each other, with an angle of 2.51° between the mean planes through their central pyrimidine rings (C9, C10, C11, C12, N4, N5 and C30, C31, C32, C33, N13, N14). Each cation was paired head-to-toe with its symmetry generated centrosymmetic twin through a coordination bond between the Cu(II) ion and the hydroxymethyl O donor of the unoccupied coordination site on the symmetry related cation (Cu1−O2A and Cu2−O4A, Figure 10). As a result, complex **8** existed as a pair of crystallographically distinct centrosymmetric dimers (Figure 11).

The coordination spheres of Cu1 and Cu2 were very similar, with only minor differences in bond lengths and angles. Cu1 was present in a tetragonally distorted

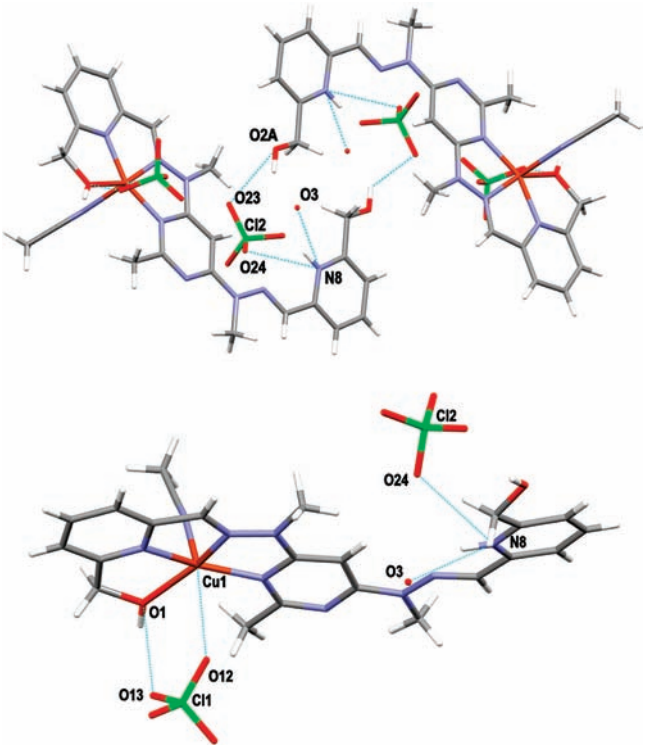

Figure 9. (Top) View of two neighboring $[Cu(\mathbf{1}H)(CH_3CN)]^{3+}$ cations joined by self-complementary H-bonding between O2−H and O23 of one of the ClO_4^- counterions. Also shown is the bifuricated H bond between N8−H and O24 and O3 (symmetry codes, A: $-x, 1-y, 1-z$). (Bottom) view of the Cl1 containing ClO_4^- positioned along the Cu1−O1 coordination bond due to a H bond between O1−H and O13 and a weak interaction between Cu1 and O12.

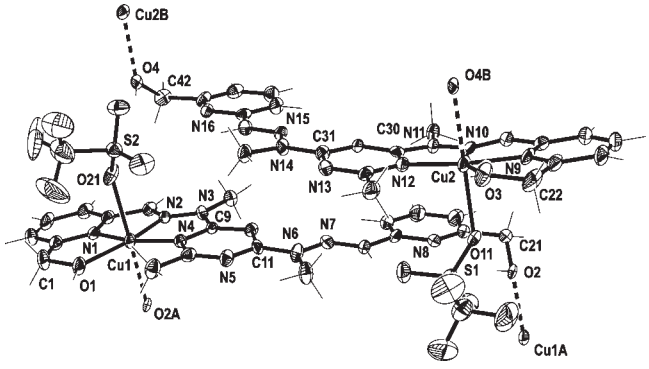

Figure 10. View of the two crystallographically distinct $[Cu\mathbf{1}(SO_3CF_3)]^+$ cation units of the asymmetric unit showing the coordination environment about the Cu(II) ion and the *cisoid* $N3_{hyz}-C9_{pym}$ and $N11_{hyz}-C30_{pym}$ bonds and the *transoid* $C11_{pym}-N6_{hyz}$ and $C32_{pym}-N14_{hyz}$ bonds (crystallographic numbering). Thermal ellipsoids drawn at the 50% probability level (symmetry codes, A: $1-x, 1-y, 1-z$; B: $-x, 1-y, 1-z$).

octahedral environment, with O1, $N1_{py}$, $N2_{hyz}$, and $N4_{pym}$ occupying the equatorial coordination sites and O21 of a $SO_3CF_3^-$ anion occupying one of the axial sites. The other axial position was occupied by the hydroxymethyl O2A donor of a symmetry generated $[Cu\mathbf{1}(SO_3CF_3)]^+$ cation. Cu2 was also present in a distorted octahedral environment, bound to the hydroxymethyl O and three N donors of a pym−hyz−py coordination pocket of the other cation of the asymmetric unit. Similarly to Cu1, the axial sites of the coordination sphere of

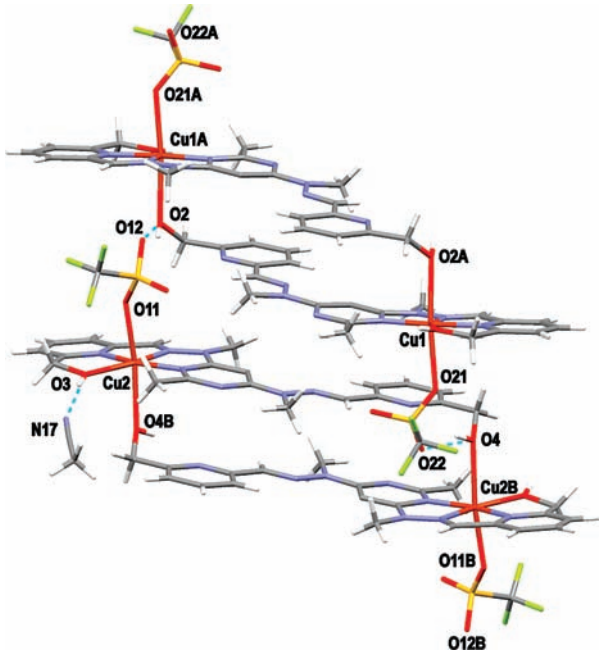

Figure 11. View of the two $[Cu\mathbf{1}(SO_3CF_3)]_2^{2+}$ cationic dimers H-bonded together through O2−H···O12 and O4−H···O22. Also shown is the CH_3CN molecule of crystallization, which is H-bonded to O3−H (symmetry codes, A: $1-x, 1-y, 1-z$; B: $-x, 1-y, 1-z$).

Cu2 were occupied by O11 of a $SO_3CF_3^-$ anion and O4A of a symmetry generated $[Cu\mathbf{1}(SO_3CF_3)]^+$ cation. Cu1 sat 0.262 Å below the mean plane of the central pyrimidine ring of its cation (C9, C10, C11, C12, N4, N5), while Cu2 sat 0.238 Å above the mean plane of the central pyrimidine ring of its cation (C30, C31, C32, C33, N12, N13).

Both of the distinct $[Cu\mathbf{1}(SO_3CF_3)]^+$ cations had a bowed shape, such that their terminal pyrimidine rings were curved away from the mean plane of the cation. For the cation that contained Cu1, the angles between the planes of the N1 and N8 containing pyridine rings and the mean plane of the cation were 6.92 and 2.78°, respectively. For the cation that contained Cu2, the angles between the planes of the N9 and N16 containing pyridine rings and the mean plane of the cation were 9.06 and 1.12°, respectively. Unlike **6** or **7**, the N donors of the unoccupied coordination sites were not protonated in either cation of complex **8**. The $N8_{py}$ and $N16_{py}$ donors were facing out from the ligand backbone of each cation, whereas in both **6** and **7**, the $N8_{py}$ donor was orientated toward the inside of the complex. Interestingly, the $N8_{py}$ and $N16_{py}$ were not involved in any significant intramolecular or intermolecular interactions

The two crystallographically distinct $[Cu\mathbf{1}(SO_3CF_3)]_2^{2+}$ dimers were held together in a head-to-toe fashion by a pair of H bonds between the $SO_3CF_3^-$ anion coordinated to the Cu(II) ion of one dimer with the hydroxymethyl arm of the unoccupied coordination site of the other dimer (Figure 11). The O2−H···O12 and O4−H···O22 distances were 2.105(7) and 2.307(8) Å, respectively [corresponding to O2···O12 and O4···O22 distances of 2.843(7) and 2.798(8) Å, respectively]. The pairing of the dimers through H-bonding resulted in an infinite 1D chain of cations running along the *a* axis (Figure 11). No $\pi-\pi$ stacking interactions were present between the $[Cu\mathbf{1}(SO_3CF_3)]_2^{2+}$ dimers. The only other intermolecular

interaction was a H bond between the CH_3CN molecule and O3, which had a O3−H···N17 distance of 1.846(11) Å [corresponding to a O3···N17 distance of 2.639(11) Å].

Comparison of the Ligand and Its Metal Complexes

Electronic Spectroscopy. In all cases, the d−d transitions of the Cu(II) complexes were represented by a single, broad, featureless peak in the UV−visible spectra, making assignment of the Cu(II) stereochemistry difficult.[38,41] Interpretation of the UV−visible spectra for the dinuclear linear complexes, $Cu_2\mathbf{1}(ClO_4)_4$ and $Cu_2\mathbf{1}(SO_3CF_3)_4$, was complicated further as their solid state structures (**4** and **5**, respectively) both included one Cu(II) ion in a tetragonally distorted octahedral geometry, while the other Cu(II) ion adopted a distorted trigonal bipyramidal geometry. The λ_{max} values of 691 and 699 nm that were observed for the two complexes, respectively, were typical of Cu(II) in a trigonal bipyramidal environment;[38,42] however, they were still within the wide range of values seen for tetragonally distorted octahedral CuN_xL_y chromophores.[38,41,43−46] The mononuclear $Cu\mathbf{1}(SO_3CF_3)_2$ complex showed a single broad peak at 679 nm, which also tentatively suggested an elongated tetragonally distorted Cu(II) stereochemistry. The mononuclear $Cu(\mathbf{1}H)(ClO_4)_2$ complex yielded two isomeric solid state structures, **6** and **7**, which contained a Cu(II) ion in a elongated tetragonal octahedral geometry and a distorted square pyramidal geometry, respectively. The peak at 657 nm was typical for Cu(II) in a distorted square pyramidal environment,[41,47] but it also fell within the wide range of values for tetragonally distorted octahedral Cu(II) geometries. Thus, the stereochemistries of the Cu(II) ion in solution could not be ascertained.

X-Ray Crystallography. X-ray crystallography confirmed that coordination of Cu(II) ions caused the pym−hyz bonds of **1** to rotate from a *transoid* to a *cisoid* conformation. In its free state, **1** was a horseshoe-shaped ligand with a distance of 6.73 Å between the centroids of its terminal pyridine rings. This distance increased significantly to 12.59 and 12.67 Å upon coordination with a two molar equivalence of Cu(II) ions to make the linear dinuclear complexes **4** and **5**, respectively. These lengths were similar in magnitude to those of other dinuclear pym−hyz complexes which contained Pb(II) and Zn(II) ions.[5] Complexes **6**, **7**, and **8** on the other hand only contained one Cu(II) ion per ligand and consequently only the pym−hyz bond of the occupied coordination site was in a *cisoid* conformation, while the pym−hyz bond of the empty coordination site retained a *transoid* shape. This is in contrast to previous studies where the reaction of larger metals such as Pb(II), Zn(II), Hg(II), and Ag(I) with pym−hyz strands on a 1:1 metal/ligand ratio resulted in [2 × 2] grid[5,9,10] and double helical[7] structures. Examples of pym−hyz strands forming grids with Cu(II) ions are rarer,[23] despite the fact that Cu(II) is commonly used in the self-assembly of [2 × 2] grids due to its flexible coordination sphere and its small crystal field stabilization energy (CFSE) which does not inhibit grid formation.[38,48,49] However, the coordination number of Cu(II) is typically restricted to 4, 5, or 6, and the addition of the hydroxymethyl arm makes the coordination pocket on **1** tetradentate, leaving only the axial coordination sites on Cu(II) available. In this way the terminal 6-hydroxymethyl substituent exerted control over the self-assembly of the mononuclear complexes **6**, **7**, and **8**.[48−50] Ligand **1** could still potentially be used to synthesize grids with larger metals such as Pb(II), which can support coordination numbers above six.[51] Additionally, the half extended complexes **6**, **7**, and **8** could possibly be utilized as intermediate structures in the stepwise assembly of heterometallic grids,[52−54] if the hydroxymethyl arm could be displaced from the Cu(II) ion. This seemed feasible as **4** and **5** showed that the hydroxymethyl arm was not always coordinated to the Cu(II) ion.

Complexes **4** to **8** exhibited a range of Cu(II) geometries, including elongated tetragonal octahedral, distorted trigonal bipyramidal, and distorted square pyramidal. Interestingly, the two Cu(II) ions in both **4** and **5** had different geometries, despite the coordination pockets they occupied being equivalent. In both **4** and **5**, one of the Cu(II) ions was present in a elongated tetragonal octahedral geometry and bound to the hydroxymethyl OH donor while the other Cu(II) ion was not bound to the O donor and adopted a distorted trigonal bipyramidal geometry. Additionally, in **5**, the tetragonally distorted octahedral Cu(II) ion was bound to two $SO_3CF_3^-$ anions, whereas the distorted trigonal bipyramidal Cu(II) was bound to two solvent molecules instead. The Cu(II) ions present in complexes **6**, **7**, and **8** were all bound to a hydroxymethyl O donor. As expected, $SO_3CF_3^-$ proved to be a stronger coordinating anion than ClO_4^-, with **5** and **8** showing coordination between $SO_3CF_3^-$ and Cu(II). Complex **6** was the only one containing ClO_4^- anions coordinated to Cu(II), while in **4** and **7** the coordination geometries of the Cu(II) ions were completed by CH_3CN solvent molecules instead. The use of $Cu(ClO_4)_2\cdot 6H_2O$ also led to the protonation of the $N8_{py}$ donor of the empty coordination site in complexes **6** and **7**. Complex **8**, which was synthesized using $Cu(SO_3CF_3)_2\cdot 4H_2O$ was not protonated, and the $N8_{py}$ and $N16_{py}$ donor atoms of the empty coordination sites were not involved in any significant intra- or intermolecular interactions.

(41) Hathaway, B. J. *J. Chem. Soc., Dalton Trans.* **1972**, 1196–1199.
(42) Murakami, T.; Takei, T.; Ishikawa, Y. *Polyhedron* **1996**, *16*(1), 89–93.
(43) Comba, P.; Lang, C.; Lopez de Laorden, C.; Muruganantham, A.; Rajaraman, G.; Wadepohl, H.; Zajaczkowski, M. *Chem.—Eur. J.* **2008**, *14*, 5313–5328.
(44) Murakami, T.; Hatakeyama, S.; Igarashi, S.; Yukawa, Y. *Inorg. Chim. Acta* **2000**, *310*, 96–102.
(45) Comba, P.; Hauser, A.; Kerscher, M.; Pritzkow, H. *Angew. Chem., Int. Ed. Engl.* **2003**, *42*, 4536–4540.
(46) Belousoff, M. J.; Tjioe, L.; Graham, B.; Spiccia, L. *Inorg. Chem.* **2008**, *47*, 8641–8651.
(47) Kruszynski, R.; Kuźnik, B.; Bartczak, T. J.; Czakis-Sulikowska, D. *J. Coord. Chem.* **2005**, *58*, 165–173.
(48) Dawe, L. N.; Shuvaev, K. V.; Thompson, L. K. *Chem. Soc. Rev.* **2009**, *38*, 2334–2359.
(49) Dawe, L. N.; Thompson, L. K. *Dalton Trans.* **2008**, 3610–3618.
(50) Hausmann, J.; Brooker, S. *Chem. Commun.* **2004**, 1530–1531.
(51) Harrowfield, J. *Helv. Chim. Acta* **2005**, *88*, 2430–2432.
(52) Bassani, D. M.; Lehn, J.-M.; Fromm, K.; Fenske, D. *Angew. Chem., Int. Ed. Engl.* **1998**, *37*(17), 2364–2367.
(53) Uppadine, L. H.; Gisselbrecht, J.-P.; Kyritsakas, N.; Nättinen, K.; Rissanen, K.; Lehn, J.-M. *Chem.—Eur. J.* **2005**, *11*, 2549–2565.
(54) Uppadine, L. H.; Lehn, J.-M. *Angew. Chem., Int. Ed. Engl.* **2004**, *43*, 240–243.

The terminal hydroxymethyl groups were involved in a variety of hydrogen bonding interactions which gave rise to supramolecular structures such as dimers (**4** and **7**) and 1D chains (**6** and **8**). Additionally, the orientation of the pyridine ring in the empty pym−hyz−py coordination site in complexes **6**, **7**, and **8** was influenced by the interactions of the hydroxymethyl O donor atom of that site. In complexes **6** and **7**, the pyridine ring was rotated such that the $N8_{py}$ donor atom pointed in toward the central pyrimidine ring of the complex as a result of the terminal OH group being H-bonded to a ClO_4^- anion located near the empty site. In complex **8**, the pyridine ring of the empty site retained the conformation seen in the free ligand, with the pyridine N donor on the outside of the ligand, due to the OH group being coordinated to a symmetry related Cu(II) ion.

Conclusion

The synthesis of ligand **1** shows that hydroxymethyl groups can be added to the terminal ends of an otherwise chemically inert pym−hyz strand to extend its versatility. Structural analysis revealed that coordination of **1** with $Cu(ClO_4)_2 \cdot 6H_2O$ and $Cu(SO_3CF_3)_2 \cdot 4H_2O$ on a 1:2 molar ratio resulted in an expansion from the horseshoe-shaped free ligand to linear dicopper complexes. This uncoiling action, brought about by the rotation of the pym−hyz bonds from a *transoid* to *cisoid* conformation, resulted in an increase in the length of the ligand from 6.73 Å to 12.59 and 12.67 Å for the ClO_4^- and $SO_3CF_3^-$ complexes, respectively. Coordination of the hydroxymethyl arm inhibited the formation of a [2 × 2] grid when **1** was reacted with the Cu(II) salts in a 1:1 molar ratio, resulting in bent complexes, where only one of the coordination sites was occupied with a Cu(II) ion and the other site was left empty. In this way, the hydroxymethyl functional groups of the terminal pyridine rings controlled the outcome of the self-assembly between ligand **1** and the Cu(II) ions.

The Cu(II) ions in the complexes showed a variety of coordination geometries, and all the complexes showed some coordination between the terminal OH groups and the Cu(II) ions. Various H-bonding interactions resulted from the OH groups, which created different supramolecular patterns such as dimers and 1D chains. It is envisioned that the terminal OH groups provide a route to incorporating pyrimidine−hydrazone molecular strands into larger molecules, so that their metal-induced, dynamic structural change could be applied to nanoscale mechanical devices.

Acknowledgment. We thank the Department of Chemistry, University of Otago and the New Economic Research Fund of the Foundation for Research, Science and Technology (NERF Grant No UOO-X0808) for financial support.

Supporting Information Available: X-ray data in CIF format and selected bond length and angle data. This material is available free of charge via the Internet at http://pubs.acs.org.